

# Recent results from the AMS/IBA laboratory at the Comenius University in Bratislava: preparation of targets and optimization of ion sources

Pavel P. Povinec<sup>1</sup> · Jozef Masarik<sup>1</sup> · Miroslav Jeřkovský<sup>1</sup> · Robert Breier<sup>1</sup> ·  
Jakub Kaizer<sup>1</sup> · Ján Pánik<sup>1</sup> · Marta Richtáriková<sup>1</sup> · Jaroslav Staníček<sup>1</sup> ·  
Alexander Šivo<sup>1</sup> · Jakub Zeman<sup>1</sup>

Received: 12 June 2015 / Published online: 27 August 2015  
© Akadémiai Kiadó, Budapest, Hungary 2015

**Abstract** Developments of solid targets and optimizations of ion sources were carried out with the aim to produce high ion yields for applications of tandem accelerators as mass spectrometers. A comparison of Al<sup>-</sup> yields from different aluminum targets showed that the best results were obtained with AlN targets. Transmission studies of <sup>9</sup>Be and <sup>12</sup>C ions through the Pelletron accelerator showed highest efficiencies for <sup>9</sup>Be<sup>2+</sup> and <sup>12</sup>C<sup>2+</sup>. First results obtained with a simplified version of the AMS line are presented as well.

**Keywords** Accelerator mass spectrometry (AMS) · Ion beam analysis (IBA) · Tandem accelerator · Pelletron · CENTA

## Introduction

Nuclear physics research, especially development of tandem accelerator technologies has had important impact on applications of small accelerators in environmental, biomedical and material sciences. The recent developments in accelerator technologies for AMS and IBA analyses have been an inspiration for creation of a Centre for Nuclear and Accelerator Technologies (CENTA) at the Comenius University in Bratislava (Slovakia). A state-of-the-art tandem accelerator laboratory has been designed for (i) AMS studies of long-lived radionuclides in

environmental, life and space sciences, (ii) IBA applications in environmental, life and material research, including cultural heritage studies, (iii) nuclear reaction studies with charged particles for new generations of fission reactors, for thermonuclear reactors, and for astrophysics investigations.

The AMS analyses of long-lived radionuclides [1–12] represent the most important development in radioanalytical techniques since the development of HPGe detectors and their operation in underground laboratories [7, 11, 13–15]. The AMS technology has been widely used in environmental studies, both terrestrial and marine. Specific applications included tracing of long-lived radionuclides (<sup>10</sup>Be, <sup>14</sup>C, <sup>36</sup>Cl, <sup>129</sup>I, U-isotopes, etc.) in climate change, atmospheric, hydrology, marine, geology and geophysics studies [2, 10, 16–19]. Some of the cosmogenic radionuclides (e.g. <sup>10</sup>Be, <sup>14</sup>C, <sup>26</sup>Al, <sup>36</sup>Cl, <sup>41</sup>Ca, <sup>53</sup>Mn, etc.) have been widely applied in space research, e.g. in analysis of meteorites and lunar samples [7, 20–23]. The AMS technology has also been frequently used in radioecology research, e.g. in atmospheric radioactivity monitoring (e.g. <sup>14</sup>C, <sup>129</sup>I, U and Pu isotopes, etc.) around nuclear reprocessing and nuclear power plants [24–26]. Actinides (U and Pu isotopes), and other long-lived radionuclides on the other hand have been playing an important role in the case of nuclear accidents (e.g. the Chernobyl accident), in long-term storage of radioactive wastes, or their dumping in the sea (e.g. <sup>14</sup>C, <sup>129</sup>I, <sup>135</sup>Cs, etc.) [9, 10, 27–29].

Recently the AMS techniques have been widely applied in tracing radionuclides released during the Fukushima accident to the terrestrial and marine environments [30]. Except the most frequently studied <sup>134</sup>Cs and <sup>137</sup>Cs (gamma-ray emitters easily measured with HPGe detectors [31, 32]), which have been important for delivery of post-accident radiation doses to the public and biota [33], there

✉ Pavel P. Povinec  
povinec@fmph.uniba.sk

<sup>1</sup> Department of Nuclear Physics and Biophysics, Faculty of Mathematics, Physics and Informatics, Comenius University, 84248 Bratislava, Slovakia

have been many other radionuclides released during the accident [30, 34–36], requiring our attention. This has been motivated first of all because of delivery of radiation doses to the public and biota by long-lived radionuclides (e.g.  $^{14}\text{C}$ ,  $^{129}\text{I}$ ,  $^{135}\text{Cs}$ , U and Pu isotopes, etc.), where especially the AMS technology (together with Inductively Coupled Plasma Mass Spectrometry (ICPMS), and Thermal Ionization Mass Spectrometry (TIMS)) has been recognized as the most sensitive analytical technique [7, 8, 10, 11, 37, 38].

The IBA technologies (e.g. PIXE, PIGE, RBS, etc.) together with the Nuclear Reaction Analysis (NRA) of environmental and material samples, and Ion Beam Modification (IBM) of materials (e.g. for construction of new generations of nuclear and thermonuclear reactors) represent the most successful applications of small accelerator technologies in various branches of science [39, 40]. The IBA technologies may also help better understanding of behavior of long-lived radionuclides in the environment via studying suitable stable elements as their analogues.

In this paper we present a short description of the CENTA laboratory, focusing on the laboratory design, description of the basic equipment and discussion of its characteristics. The first results obtained with a simplified version of the AMS line are presented as well.

## Experimental

### Description of the tandem accelerator laboratory

The CENTA laboratory because of financial constrains has been built *per partes*, comprising the main equipment required for AMS and IBA analytical work. The design of the laboratory has been driven by general needs to establish in Slovakia a national laboratory devoted to ion beam studies and applications, and to assure for the future wide-range research capabilities and successful participation in international programs. The present laboratory design comprises of two ion sources (for gas and solid targets), the injection system, the 3 MV tandem accelerator, and a high energy analyzer with two ion beam end stations for PIGE/PIXE, NRA and AMS applications. All available equipment was supplied by the National Electrostatics Corporation (NEC, Middleton, USA). A floor scheme of the tandem accelerator laboratory is presented in Fig. 1. The near future installation will include a fully equipped AMS line with  $90^\circ$  magnet, an electrostatic spectrometer, and the end of the line detector. Later installations will include a nuclear microscope, a raster station for IBM studies of materials, and a station for biomedical research.

A dedicated hall to accommodate the tandem accelerator laboratory has been built at the Comenius University

campus at Mlynská dolina. The hall design separates the ion beam channels (placed in a bunker covered by soil) from the AMS line, enabling thus work in different radiation environments (Fig. 1). Neutron and gamma-ray detectors monitor radiation situation in the main hall.

The laboratory is equipped with an Alphasource ion source (radio frequency plasma source producing ions from gases), and with MC-SNICS source (MultiCathode Source of Negative Ions by Cesium Sputtering) having a wheel accommodating up to 40 solid targets (Fig. 2). All elements, which can exist in gaseous form and can form negative ions (either atomic or molecular) could be considered candidates for ion production in the Alphasource ion source. The MC-SNICS ion source is used for production of ions from solid targets (from lithium to transuranics).

The ion beams from the Alphasource and MC-SNICS sources are forwarded to an electrostatic analyzer (ESA) with 300 mm radius of electrodes, mounted on a rotatable platform (Figs. 1, 2). The ion beams from both ion sources are chosen for analysis, where the first  $E/q$  separation is made. The X–Y steerers and slits can be used for beam tuning, attenuation and analysis before entering the injection magnet. The momentum analysis  $ME/q^2$ , and separation of ions before acceleration is made by double focusing  $90^\circ$  magnet with bending radius of 0.4572 m. The mass resolution of the injection magnet (for a 3 mm beam spot and the dispersion constant  $D_m = 4$ ) is  $m/\Delta m = 305$ . After the proper mass is selected, another set of slits is used for parameterization of the beam, and a Faraday cup is used for measurements of ion currents. Negative ion beams produced in Alphasource or MC-SNICS ion sources, pre-accelerated to modest energies (40–100 keV), are then injected into the tandem accelerator.

A 3 MV tandem electrostatic accelerator (NEC Pelletron Model 9SDH-2) can accelerate a variety of ion species over a broad range of energies for use in AMS, IBA, IBM, and nuclear physics/astrophysics studies. The terminal is provided with a gas (presently nitrogen) stripping system. The energy of accelerated ions depends mainly on the terminal voltage and on the charge state of accelerated ions. The accelerator is housed in a pressure vessel (diameter of 1.22 m and length of 5.64 m), which allows an evacuation and subsequent filling with sulphur hexafluoride ( $\text{SF}_6$ ) insulating gas required for high voltage operation. A cryogenic-vacuum/pressure apparatus used for the evacuation, transport and storage of  $\text{SF}_6$  gas has been supplied by the DILO company (Germany).

The ions accelerated in the Pelletron are then focused in the high-energy beam line with a magnetic quadrupole triplet lens, and a Y-axis electrostatic steerer (Figs. 1, 2). The quadrupole magnet is primarily used for IBA and NRA applications. The switching magnet, presently also used as an analyzing magnet for AMS ( $ME/Z^2 = 300 \text{ amu-MeV}$

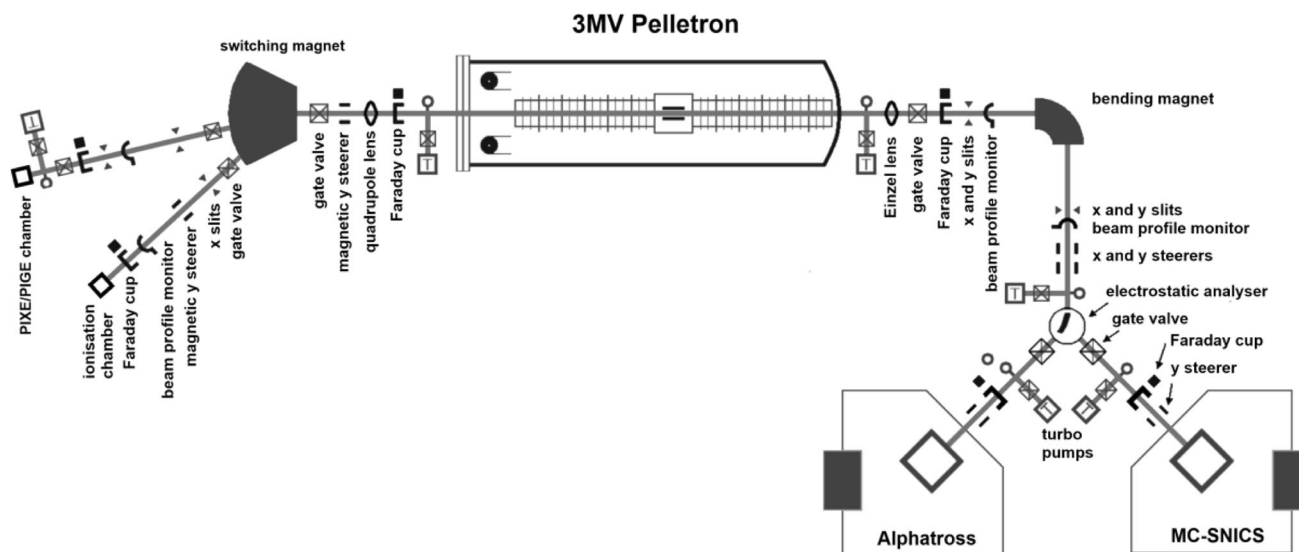


**Fig. 1** Floor scheme of the tandem accelerator laboratory

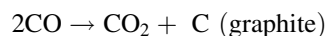
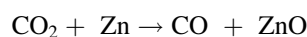
@  $\pm 15^\circ$ ), is equipped with seven ports at  $\pm 45^\circ$ ,  $\pm 30^\circ$ ,  $\pm 15^\circ$ , and  $0^\circ$  with respect to the accelerator. The beam lines from these ports will be used for IBA (channeling, RBS, PIXE, PIGE), IBM, nuclear reaction studies, nuclear microscope and for biomedical applications. The  $+45^\circ$  and  $+15^\circ$  beam lines are currently equipped with slits to control the divergence of the ion beam, with X–Y electromagnetic steerers, with Faraday cups for current measurements and with beam profile monitors. A PIXE/PIGE end station has been installed at the  $+15^\circ$  port. The other end of the line detectors (an ionization chamber, silicon detector, time of flight detector) for the total energy analysis of ions, for analysis of their energy losses and their residual energy will also be installed soon. The switching magnet can also be used to select the energy and charge state of the ions to be delivered to the end station as a dedicated beam line for AMS analysis will be installed later.

### Preparation of graphite targets for $^{14}\text{C}$ analysis by AMS

A vacuum-cryogenic apparatus was constructed to produce  $\text{CO}_2$  either by combustion of samples in oxygen atmosphere, or by acid evolution (Fig. 3). The graphitization apparatus is located in a clean laboratory dedicated for preparation of radiocarbon samples. The line is made of borosilicate glass and is used for extraction of  $\text{CO}_2$  from various samples, e.g. groundwater, seawater, solid carbonates and organic samples. The line has an advantage in

extracting carbon dioxide and its graphitization in the same place, what substantially lowers a risk of contamination. The vacuum in the line can go down to  $\sim 10^{-5}$  torr with the use of rotary and diffusion pumps. The  $\text{CO}_2$  after its extraction from samples is purified by passing through water vapor traps kept at  $-45^\circ\text{C}$  and silver (wool) plus copper (granules) furnaces heated to about  $900^\circ\text{C}$ . After the purification the  $\text{CO}_2$  is then injected into the graphitization reactor. Precisely known volumes of the pure  $\text{CO}_2$  were then reduced to graphite in four graphite reactors.

We compared two graphitization procedures: one is using for the graphitization reaction Zn and Fe [41], the second method is using externally supplied hydrogen from a gas cylinder [42]. In the first reaction



the reduction was carried out with Zn in the presence of dendritic Fe (200 mesh). Both chemicals were carefully weighed and introduced into the glass tubes. They were then connected to the graphite apparatus, together with a tube filled with purified  $\text{CO}_2$  extracted from a sample. The air above was pumped out and the  $\text{CO}_2$  was transferred cryogenically to the reactor. The Zn tube was then heated to  $450^\circ\text{C}$ , which pre-reduced  $\text{CO}_2$  to CO. After 1 h, the Fe was heated to  $550^\circ\text{C}$  and graphite was produced and deposited onto the Fe. The pressure was constantly monitored until the reaction was completed, which usually takes between 8 and 10 h. The produced graphite was then carefully weighed.





**Fig. 2** View of the main components of the tandem laboratory. **a** Alphasource (left) and MC-SNICS ion sources (right); **b** Injection line; **c** Pelletron accelerator with control system; **d** Ion analyzer with switching magnet and ion beam lines

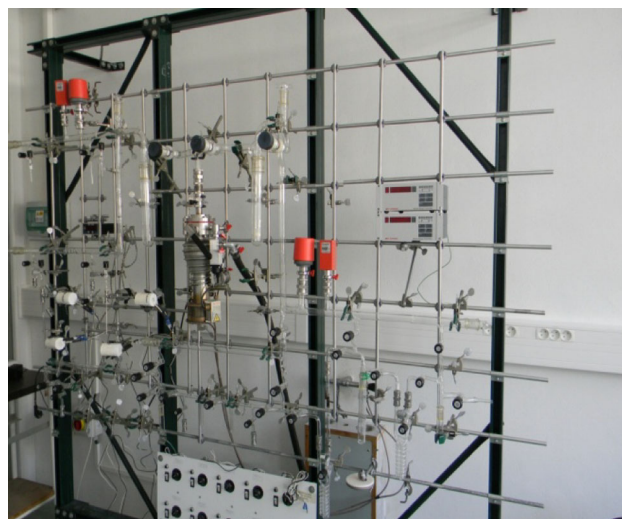
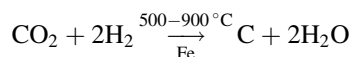


**Fig. 3** Combustion-graphitization line for preparation of  $^{14}\text{C}$  targets for AMS measurements

The second method is based on the following reaction [42]:



A graphitization reactor is comprised of a reaction tube (with the iron catalyst inside), heated with an electric oven, a water trap (a tube cooled with methanol and liquid nitrogen to about  $-45^\circ\text{C}$ ) and a pressure transducer (for monitoring of the pressure during the graphitization). There are four graphitization reactors altogether. High-purity iron powder (325 mesh) is used as the catalyst. An appropriate amount of Fe catalyst is weighed in a reaction tube mounted to a graphitization reactor, which is then pre-heated in the presence of hydrogen. Hydrogen gas (purity of 99.9 %) used for the catalyst activation and graphitization itself, originates from an external gas bottle. The amount of hydrogen used for graphitization equals approximately double the amount of the  $\text{CO}_2$  sample. Typically, the reaction is ended in less than 4 h with a yield of 98 %, which is calculated from the pressure decline during the reaction, and also confirmed gravimetrically.

## Results and discussion

Several studies have been carried out till now in the CENTA laboratory, including investigations of characteristics of ion sources, ion transmission efficiency studies [43, 44], optimization of ion yields from  $\text{UF}_4$  and UO targets for analysis of uranium isotopes by AMS [25], analysis of  $^{10}\text{Be}$  by AMS [43], development of  $^{14}\text{C}$  and  $^{129}\text{I}$  targets for AMS analyses [44, 45], and  $^{14}\text{C}$  analysis in

single tree-ring samples [25, 45]. Here we shall focus only on a few recent results.

### Comparison of methods for preparation of graphite targets

The full procedure of preparation of graphite targets was tested by burning several samples of the oxalic-acid standard reference material (HOxII, NIST SRM 4990C) of the National Institute of Standards and Technology's (Gaithersburg, USA). The graphite yields as obtained by both methods were calculated gravimetrically and also barometrically from pressure readings. In the case of the first method about 2 mg of carbon was found to be the appropriate amount for synthesis. For complete reduction, the pressure should drop to zero, meaning all gaseous CO<sub>2</sub> and CO has been reduced to solid graphite. Figure 4, depicting the variation of pressure with time, shows that a successful synthesis with a yield of about 98 % was reached. Sometimes a lower synthesis, with a yield of about 95 % was reached, as the curve did not return to a zero pressure state, probably because of the presence of water vapors in the system. The mass of Fe used, enabling to reach an acceptable ionic current in the AMS source, was twice the amount of carbon that needed to be reduced.

Several parameters, including reactor volume, amount of iron catalyst and its type, temperature and catalyst activation conditions were studied in the hydrogen method with the aim to reduce a reaction time and increase a final yield of the graphitization. Increasing the reactor volume from 9.1 ml to 18.2 enhanced the yield by about 6 %, and shortened the reaction time by about 80 min. Varying of the Fe catalyst amount has little or no effect, an optimal value was set between 4 and 6 mg. It has been found that

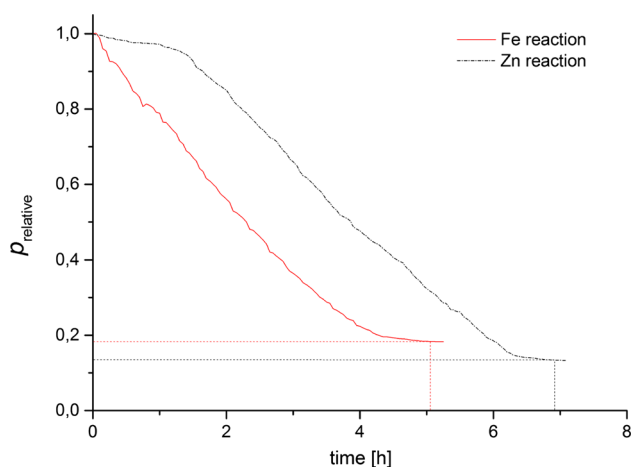


**Fig. 4** Comparison of pressure–time records obtained with different graphitization methods (*top line* a reactor without external hydrogen; *bottom line* a reactor with external hydrogen)

the first step of the overall reaction—the reduction of CO<sub>2</sub> to CO—has improved if done at higher temperature, i.e. 900 °C. After 0.5 h the temperature is lowered to 550 °C for the rest of the graphitization. Heating of the iron powder in the presence of hydrogen (600 °C, 1 h) was chosen as our standard catalyst activation procedure, though if compared to heating in the open atmosphere and vacuum respectively, the yield and time difference was rather small.

Figure 4 compares history of two graphitization processes, with and without external supply of hydrogen, expressed as the reactor pressure and the reaction time. It is clearly seen that the optimization in the hydrogen procedure resulted in a much faster reaction (below 4 h), and slightly increased yield up to 98 %. Therefore, the method with external hydrogen has been routinely used for preparation of graphite targets for AMS <sup>14</sup>C measurements.

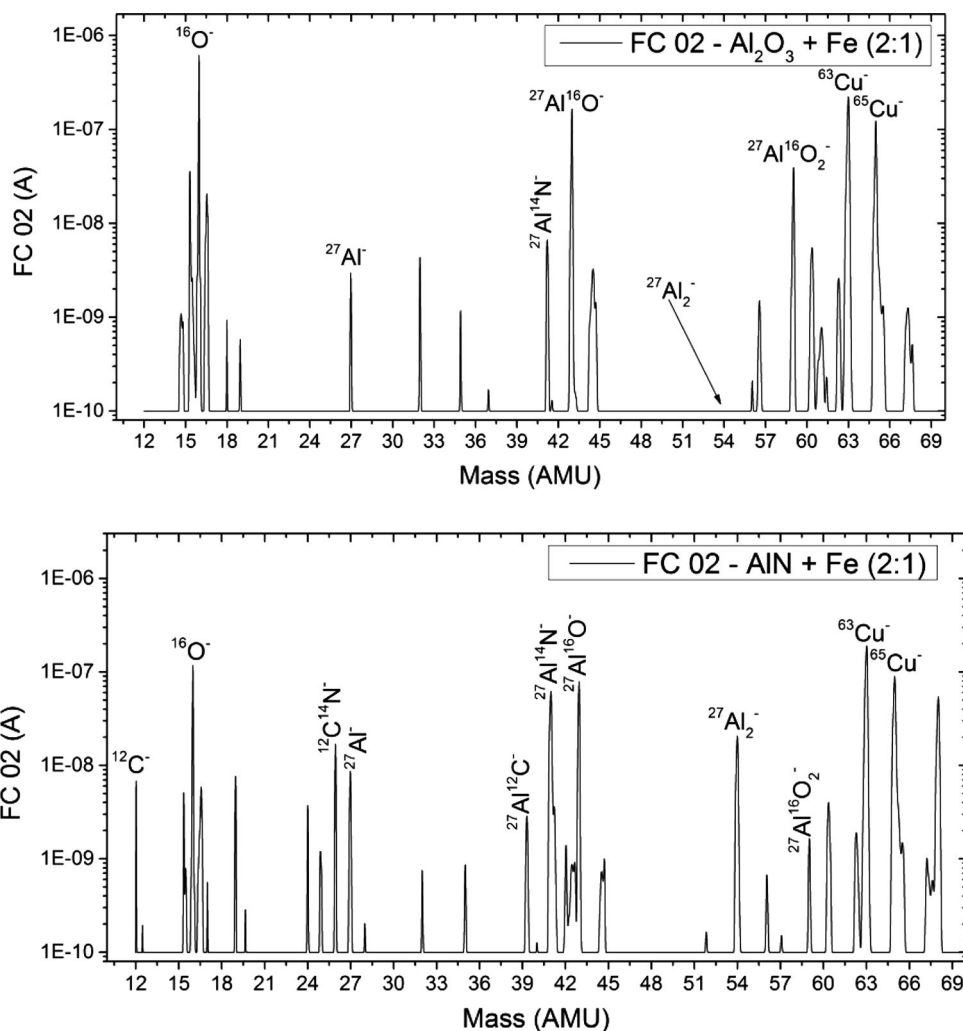
### Investigation of aluminum targets for AMS analysis

Different aluminum samples were tested as possible targets in the MC-SNICS ion source for preparation of Al ions for <sup>26</sup>Al measurements by AMS. It is well known that aluminum does not have high yields of negative ions as for example chlorine, carbon or beryllium. As it is disadvantageous to use metallic aluminum in the ion source (e.g. in the form of aluminum powder, wires or sheets) because of low ion yields, synthesized targets should be prepared. The Al<sub>2</sub>O<sub>3</sub> target could be a compromise because it is stable at high temperatures used in the ion source, it is not toxic, it is stable on the air, and relatively easy to be prepared from geological or biological samples. However, there are also disadvantages, e.g. a high concentration of oxygen, and a high electrical resistance of the oxide. Therefore it should be mixed with good conductor, e.g. iron, copper or silver.

On the other hand AlN could be a promising target material as it could produce higher ion yields, and as nitrogen does not form negative ions, it should not interfere with production of Al<sup>−</sup> ions. The disadvantages of AlN include more complicated preparation chemistry (an air-free Schlenk-type technique), its sensitivity to water vapors (formation of AlOH<sub>3</sub>), and lower electrical conductivity [46, 47].

Several aluminum samples (Al<sub>2</sub>O<sub>3</sub>, AlF<sub>3</sub>, AlN, and Al<sub>2</sub>SO<sub>4</sub>) were tested in the MC-SNICS ion source with the aim to study Al<sup>−</sup> ion yields. A comparison of mass spectra obtained with Al<sub>2</sub>O<sub>3</sub> and AlN targets mixed with Fe powder at the ratio 2:1 shows that the best yields have been obtained with the AlN target (Fig. 5). Lower Fe mixing ratios, or mixing of the targets with Cu or Ag (for getting a better thermal and electric conductivity) gave lower yields. In both mass spectra we also see <sup>63</sup>Cu and <sup>65</sup>Cu peaks from the copper cathode in which Al + Fe mixtures were

**Fig. 5** Comparison of mass spectra of the  $\text{Al}_2\text{O}_3$  and  $\text{AlN}$  targets mixed with Fe powder



pressed. The peak with mass of 26 seen in the  $\text{AlN}$  mass spectrum is not due to the radioactive  $^{26}\text{Al}$  for which we are looking for in AMS measurements, but this is interference from  $^{12}\text{C}^{14}\text{N}^-$ .

### Transport of ions through the accelerator system

The Alphasross and MC-SNICS ion sources were optimized for IBA and AMS operations, including studies of transmission characteristics of accelerated ions with different energy and charge states. The nitrogen gas pressure in the gas stripper has been optimized for different ions and charge states. For example, the maximum transmission efficiencies at 3 MV obtained for  $^9\text{Be}^{1+}$ ,  $^9\text{Be}^{2+}$  and  $^9\text{Be}^{3+}$  ions used for AMS measurements of  $^{10}\text{Be}$  were about 30, 52 and 5 %, respectively (Fig. 6). The  $^9\text{Be}^{2+}$ -beam tuned to the end Faraday cup had the diameter of 2 mm.

In the case of  $^{12}\text{C}$  ions the maximum transmission efficiencies at 3 MV obtained for  $^{12}\text{C}^{2+}$ ,  $^{12}\text{C}^{3+}$ ,  $^{12}\text{C}^{4+}$  and

$^{12}\text{C}^{5+}$  were about 45, 33, 23 and 0.6 %, respectively (Fig. 6).

### AMS analysis of $^{10}\text{Be}$ standard and background samples

As an example of the first AMS measurements carried out at the CENTA facility we present an analysis of  $^{10}\text{Be}$  [48]. AMS analysis of  $^{10}\text{Be}$  using only a small switching magnet as the ion analyzer (Fig. 1) was tested. The method for suppression of  $^{10}\text{B}$  ions, based on a silicon nitride foil stack used as a passive absorber was developed earlier at the VERA laboratory. The AMS analysis of  $^{10}\text{Be}$  is mainly limited by the stable isobar  $^{10}\text{B}$ , while the requirements for mass separation are the least stringent of all standard radionuclides analyzed by AMS. The MC-SNICS was used for the production of  $^{10}\text{BeO}^-$  ions, which were mass separated and injected into the 9SDH-2 Pelletron, operating at 3 MV terminal voltage. As already mentioned, the  $^{10}\text{Be}^{2+}$



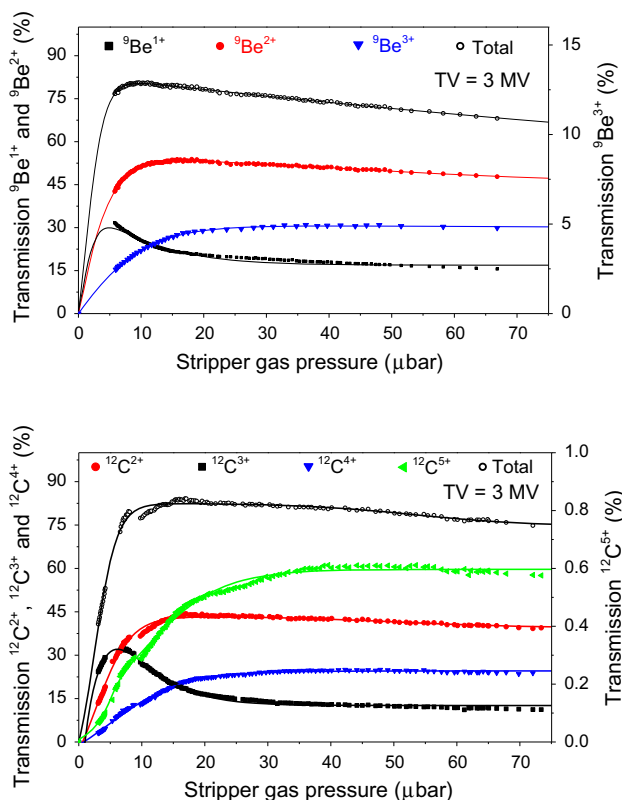


**Fig. 6** Transmission of  $^9\text{Be}$  and  $^{12}\text{C}$  ions on the stripper gas ( $\text{N}_2$ ) pressure at the terminal voltage of 3 MV

ions were selected for analysis because of highest transmission efficiency. The  $^{10}\text{B}$  ions, as well as of most background ions from heavier masses were absorbed in the silicon nitride stack introduced in front of the ion detection chamber consisting of two anodes (based on the ETH Zürich design [49]), which was used for the ion detection. The standard  $^{10}\text{Be}$  source (S555 developed at ETH Zürich [50]) with the  $^{10}\text{Be}/^9\text{Be}$  mass ratio of  $(8.71 \pm 0.24) \times 10^{-11}$  was used in these measurements. Using this setup, a detection limit for  $^{10}\text{Be}/^9\text{Be}$  of the order of  $10^{-12}$  was achieved, which was mainly determined by scattering of  $^9\text{Be}^{2+}$  ions (energy of 7.059 MeV) on residual gas inside the switching magnet.

## Conclusions

The ion sources, the Pelletron accelerator and the analyzer of accelerated ions installed in the CENTA laboratory have been described. Preliminary results indicated a reliable operation of all parts of the system. A vacuum-cryogenic apparatus has been constructed and a method for preparation of graphite targets for  $^{14}\text{C}$  AMS analysis has been developed. It has been shown that the method using external hydrogen for graphitization of samples has been

faster and more reliable than the Zn method. A comparison of  $\text{Al}^-$  yields from different aluminum targets in the MC-SNICS ion source showed that the best results were obtained with  $\text{AlN}$  and  $\text{Al}_2\text{O}_3$  targets mixed with iron powder at the ratio of 2:1. Transmission studies of  $^9\text{Be}$  and  $^{12}\text{C}$  ions on the pressure of nitrogen gas in the gas stripper of the Pelletron accelerator and on the charge states of the ions showed that the highest efficiencies were obtained for  $^9\text{Be}^{2+}$  (52 %) and  $^{12}\text{C}^{2+}$  (45 %). A simplified system for AMS analysis of  $^{10}\text{Be}$  using the switching magnet (as the analyzing magnet) and an ionization chamber with a silicon nitride stack absorber for  $^{10}\text{B}$  isobar suppression achieved a detection limit for  $^{10}\text{Be}/^9\text{Be}$  mass ratio of the order of  $10^{-12}$ .

A wide range of samples were used for  $^{14}\text{C}$  AMS analysis including, atmospheric  $\text{CO}_2$ , tree-ring, groundwater, seawater, sediment, canvas, pergamon, charcoal, mortar, and bone samples. It is planned that a complete AMS line will also be available soon. The scientific program of the CENTA will be devoted mainly to nuclear, environmental, material and life sciences.

**Acknowledgments** A support provided by the EU Research and Development Operational Program funded by the ERDF (projects Nos. 26240120012, 26240120026 and 26240220004) has been crucial for establishing the CENTA laboratory. The authors are also acknowledging support from the Technical Cooperation Program of the International Atomic Energy Agency (project No. SLR/0/008), and from the Nuclear Regulatory Authority of the Slovak Republic. They are also indebted to Profs. R. Golsner, A. Priller, and P. Steier of the Vienna University for support during development of the AMS system. The staff of the Comenius University is acknowledged for assistance during various stages of preparation and building of the CENTA laboratory.

## References

1. Tuniz C, Bird JR, Fink D, Herzog GF (1998) Accelerator mass spectrometry: ultrasensitive analysis for global science. CRC Press, Boca Raton
2. Kutschera W (2005) Intern J Mass Spectrom 242:145–160
3. Povinec PP (2005) J Radioanal Nucl Chem 263:413–417
4. Povinec PP, Sanchez-Cabeza JA (eds) (2006) Radionuclides in the environment. Elsevier, Amsterdam
5. Povinec PP (ed) (2008) Analysis of environmental radionuclides. Elsevier, Amsterdam
6. Povinec PP (2008) J Radioanal Nucl Chem 276:771–777
7. Povinec PP, Betti M, Jull AJT, Vojtyla P (2008) Acta Phys Slovaca 58:1–154
8. Lee SH, Povinec PP, Gastaud J, La Rosa J, Wyse E, Fifield LK (2009) J Radioanal Nucl Chem 282:831–835
9. Lehto J, Hou XL (2010) Chemistry and analysis of radionuclides. Wiley, Weinheim
10. Povinec PP (2004) In: Livingston HD (ed) Marine radioactivity. Elsevier, Amsterdam
11. Povinec PP, Eriksson M, Scholten J, Betti M (2012) In: Annunziata M (ed) Handbook of radioactivity measurement. Elsevier, Amsterdam
12. Povinec PP (2013) J Radioanal Nucl Chem 295:537–544

13. Povinec PP, Comanducci JF, Levy-Palomo I (2004) *Appl Rad Isotopes* 61:85–93
14. Povinec PP, Comanducci JF, Levy-Palomo I (2005) *J Radioanal Nucl Chem* 263:441–445
15. Povinec PP (2012) *J Anal Sci Technol* 3:42–71
16. Povinec PP, Lee SH, Kwong LLW, Oregioni B, Jull AJT, Kieser WE, Morgenstern U, Top Z (2010) *Nucl Instrum Meth Phys Res B* 268:1214–1218
17. Povinec PP, Zenisova Z, Sivo A, Ogrinc N, Richtáriková M, Breier R (2013) *Radiocarbon* 55:1017–1028
18. Povinec PP, Breier R, Coppola L, Groening M, Jeandel C, Jull AJT, Kieser WE, Lee SH, Kwong LLW, Morgenstern U, Top Z (2011) *Earth Planet Sci Lett* 302:14–26
19. Fabel D, Stroeven AP, Harbor J, Kleman J, Elmore D, Fink D (2002) *Earth Planet Sci Lett* 201:397–406
20. Povinec PP, Laubenstein M, Ferrière L, Brandstätter F, Sýkora I, Kováčik A, Jull AJT, Topa D, Koeberl C (2015) *Meteor Planet Sci* 50:273–286
21. Poutitvsev M, Dillmann I, Faestermann T, Knie K, Korschinek G, Lachner J, Meier A, Rugel G, Wallner A (2010) *Nucl Instrum Meth Phys Res B* 268:756–758
22. Jull AJT, McHargue LR, Bland PA, Greenwood RC, Bevan AWR, Kim KJ, Giscard MD, LaMotta SE, Johnson JA (2010) *Meteor Planet Sci* 45:1271–1283
23. Leya I, Welten KC, Nishiizumi K, Caffee MW (2009) *Meteor Planet Sci* 44:77–85
24. Molnár M, Major I, Haszpra L, Svetlik I, Svingor E, Veres M (2010) *J Radioanal Nucl Chem* 286:471–476
25. Povinec PP, Svetlik I, Jeřkovský M, Šivo A, John J, Špendlíková I, Němec M, Kučera J, Richtáriková M, Breier R, Fejgl M, Černý R (2015) *J Radioanal Nucl Chem* 304:67–73
26. Livingston HD, Povinec PP (2000) *Ocean Coast Manag* 43:689–712
27. Steier P, Hrncsek E, Priller A, Quinto F, Srncik M, Wallner G, Winkler S (2013) *Nucl Instrum Methods Phys Res B* 294:160–164
28. Lujanienė G, Beneš P, Štamberg K, Šapolaite J, Vopalka D, Radžiute E, Ščiglo T (2010) *J Radioanal Nucl Chem* 286:353–359
29. Povinec PP, Oregioni B, Jull AJT, Kieser WE, Zhao XL (2000) *Nucl Instrum Meth Phys Res B* 172:672–678
30. Povinec PP, Hirose K, Aoyama M (2013) *Fukushima accident: radioactivity impact on the environment*. Elsevier, New York
31. Levy I, Povinec PP, Aoyama M, Hirose K, Sanchez-Cabeza JA, Comanducci J-F, Gastaud J, Eriksson M, Hamajima Y, Kim CS, Komura K, Osvath I, Roos P, Yim SA (2011) *Prog Oceanogr* 89:120–133
32. Povinec PP (2011) *J Anal Sci Technol* 2(Suppl A):A15–A21
33. Povinec PP, Hirose K (2015) *Sci Rep* 5:9016. doi:[10.1038/srep09016](https://doi.org/10.1038/srep09016)
34. Steinhäuser G (2014) *Environ Sci Technol* 48(9):4649–4663
35. Hou XL, Povinec PP, Zhang LY, Biddulph D, Chang C-C, Fan YK, Golser R, Jeskovsky M, Jull AJT, Liu Q, Shi KL, Steier P, Zhou WJ (2013) *Environ Sci Technol* 47:3091–3098
36. Povinec PP, Aoyama M, Biddulph D, Breier B, Buessler K, Chang CC, Golser R, Hou XL, Jeskovsky M, Jull AJT, Kaizer J, Nakano M, Nies H, Palcsu L, Papp L, Pham MK, Steier P, Zhang LY (2013) *Biogeosciences* 10:5481–5496
37. Lee SH, Povinec PP, Wyse E, Hotchkis MAC (2008) *Appl Rad Isotopes* 66:823–828
38. Zheng J, Tagami K, Homma-Takedaa S, Buab W (2013) *J Anal At Spectrom* 28:1676–1699
39. Jeynes C, Webb RP, Lohstroh A (2011) *Rev Accel Sci Technol* 4:41–82
40. Hosemann P (2011) *Rev Accel Sci Technol* 4:161–182
41. Liong Wee Kwong L, Povinec PP, Jull AJT (2004) *Radiocarbon* 46:133–139
42. Vogel JS, Southon JR, Nelson DE, Brown TA (1984) *Nucl Instrum Meth Phys Res B* 5:289–293
43. Povinec PP, Masarik J, Kúš P, Holý K, Jeřkovský M, Breier R, Staníček J, Šivo A, Richtáriková M, Kováčik A, Szarka J, Steier P, Priller AA (2015) *Nucl Instrum Meth Phys Res B* 342:321–326
44. Povinec PP, Masarik J, Jeřkovský M, Kaizer J, Šivo A, Breier R, Pánik J, Staníček J, Richtáriková M, Zahoran M, Zeman J (2015) *Nucl Instrum Meth Phys Res B*. doi:[10.1016/j.nimb.2015.02.021](https://doi.org/10.1016/j.nimb.2015.02.021)
45. Povinec PP, Šivo A, Jeřkovský M, Svetlik I, Richtáriková M, Kaizer J (2015) *Radiocarbon* 57:355–362
46. Flarend R et al (2004) *Nucl Instrum Meth Phys Res B* 223–224:263–267
47. Sharma P et al (2000) *Nucl Instrum Meth Phys Res B* 172:112–123
48. Jeřkovský M, Steier P, Priller A, Breier R, Povinec PP, Golser R (2015) *Nucl Instrum Meth Phys Res B*. doi:[10.1016/j.nimb.2015.04.072](https://doi.org/10.1016/j.nimb.2015.04.072)
49. Stocker M, Döbeli M, Grajcar M, Suter M, Synal H-A, Wacker L (2005) *Nucl Instrum Meth Phys Res B* 240:483–486
50. Christl M, Lachner J, Vockenhuber C, Lechtenfeld O, Stimac I, van der Loeff MR, Synal H-A (2012) *Geochim Cosmochim Acta* 77:98–107